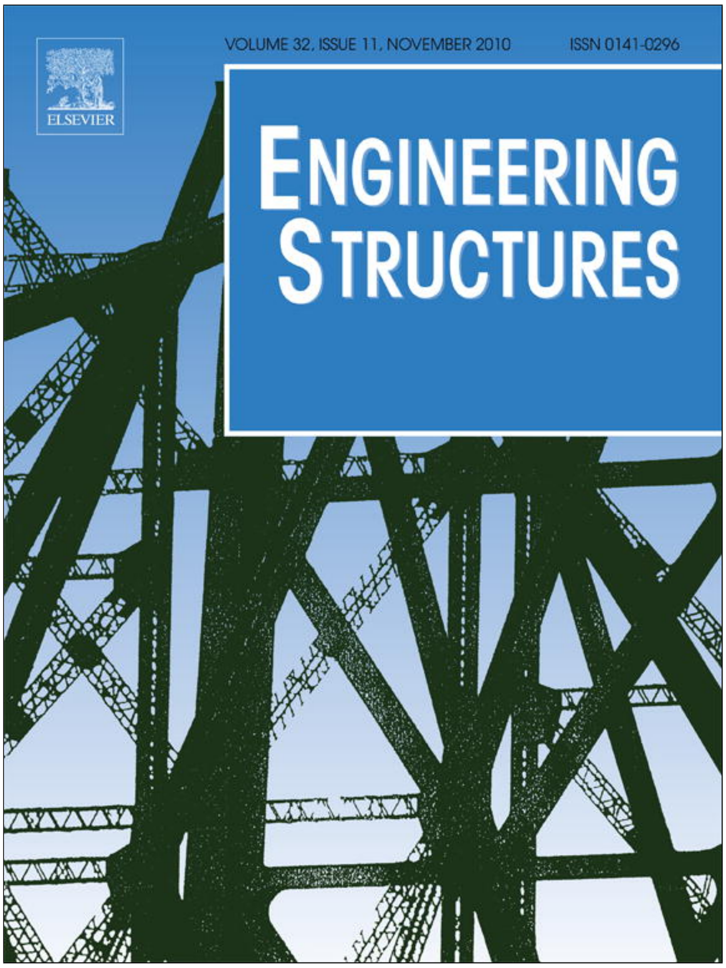
VOLUME 32, ISSUE 11, NOVEMBER 2010
ISSN 0141-0296
ELSEVIER
ENGINEERING STRUCTURES

Engineering Structures 32 (2010) 3539–3547

Contents lists available at ScienceDirect

Engineering Structures

journal homepage: www.elsevier.com/locate/engstruct

Simple design procedure of a friction damper for reducing seismic responses of a single-story structure

Kyung-Won Min [a], Ji-Young Seong [a], Jinkoo Kim [b,*]

[a] Department of Architectural Engineering, Dankook University, Yongin, South Korea

[b] Department of Architectural Engineering, Sungkyunkwan University, Suwon, South Korea

ARTICLE INFO

Article history:
Received 3 October 2009
Received in revised form
15 July 2010
Accepted 23 July 2010
Available online 15 September 2010

Keywords:
Friction dampers
Equivalent damping ratio
Dynamic magnification factors
Response reduction factor
Seismic excitation

ABSTRACT

This study proposed a simple design procedure for determining the required damping force of a friction damper installed in a single-story structure. The analysis model was transformed into an equivalent mass-spring-dashpot system by approximating a nonlinear Coulomb damping force with an equivalent viscous damping force. A closed form solution for the dynamic magnification factor (DMF) for a steady-state response was derived using the energy balance equation. The equivalent viscous damping ratio was defined using the DMF at the natural frequency. The transfer function between input harmonic excitation and output structural response was obtained from the DMF, and the response reduction factor of the root mean square (RMS) of displacements with and without friction dampers was analytically determined. Using the proposed procedure the friction force required for satisfying a given target response reduction factor was obtained. The response reduction factors were obtained for the structures with different natural frequencies subjected to ten earthquake records. Based on the dynamic analysis results, it was concluded that the mean response reduction factors matched well with the target values.

1. Introduction

Friction dampers are considered as one of the most efficient energy dissipation devices for structures against an earthquake load. Compared with velocity-dependent devices such as viscous and viscoelastic dampers, friction dampers can provide sufficient initial stiffness as well as energy-dissipation capacity. A lot of research have been carried out to investigate the energy-dissipating capacity of friction dampers and to propose a proper design procedure. Energy dissipations of slotted bolted friction dampers were investigated numerically and experimentally [1,2]. Fu and Cherry [3] studied the application of a quasi-static design procedure for a friction damped system. They also proposed a code-based seismic design procedure for friction damped frames [4]. Mualla and Belev [5] proposed a friction damping device (FDD) and carried out tests for assessing the friction pad material, damper unit performance and scaled model frame response to lateral harmonic excitation. Moreschi and Singh [6] presented a methodology to determine the optimal design parameters for the devices installed at different locations in a building for a desired performance objective. Bhaskararao and Jangid [7] proposed numerical models of friction dampers for multi degree of freedom (MDOF) structures and validated the results with those obtained from an analytical model. A new equivalent linearization technique was proposed for a friction damper–brace system based on the probability distribution of the extreme displacement [8]. Lee et al. [9–11] proposed the design methodology for a combined system of bracing and friction dampers for the seismic retrofit of structures, and assessed the vibration control effect quantitatively by evaluating the equivalent damping ratio of a structure with supplemental damping devices. Marko et al. carried out comparative studies of the response of shear wall structures with friction dampers, viscoelastic dampers and combined friction–viscoelastic dampers subjected to earthquakes [12]. They demonstrated the feasibility of mitigating the seismic structural response with embedded dampers. Ribakov demonstrated a method to improve the seismic behavior of MDOF buildings by applying a variable stiffness friction damped system [13]. Recently Kim et al. [14] investigated progressive collapse performance of structures installed with rotational friction dampers. Most of the previous studies were generally carried out by using finite element analysis tools for analysis of structures installed with friction dampers. This provides quantitative information about structural responses and damper behavior, but not insight into the physical behavior and effect of friction dampers. In this regard a simple design and performance evaluation process for friction dampers mounted on building structures are required to evaluate the effectiveness and economy of damper installation.

* Corresponding author. Tel.: +82 31 290 7563; fax: +82 31 290 7570.
E-mail address: jkim12@skku.edu (J. Kim).

0141-0296/$ – see front matter © 2010 Elsevier Ltd. All rights reserved.
doi:10.1016/j.engstruct.2010.07.022

The present study is intended to propose a simple design process to determine a desired control force of a friction damper to satisfy a given target performance of a structure subjected to an earthquake ground excitation. The energy balance of input loading and output building motion is investigated to identify the building–damper system under steady-state behavior. A closed form solution for the dynamic magnification factor (DMF) is derived by assuming that the friction damped building structure shows steady-state response, and that the Coulomb damping force can be replaced by equivalent viscous damping force. A straightforward methodology is suggested to assess the control efficiency of a friction damped building structure under an earthquake ground excitation by modifying the DMF into a transfer function. Then the response reduction factor of the root mean square (RMS) of displacements with and without friction dampers is found analytically. Finally a design procedure is proposed to determine the required damping ratio and friction force to satisfy a given target response reduction factor. Numerical dynamic analyses are carried out to check the validity of the proposed procedure.

2. Closed form solution for a dynamic magnification factor

Friction dampers are generally installed between stories to reduce inter-story displacements of structures as shown in Fig. 1. They generate damping forces characterized by Coulomb damping, the direction of which is opposite to structural motion. The equation of motion of a single-story structure with a friction damper is represented by

$$m\ddot{u} + c_v\dot{u} + ku + f_d \text{sgn}(\dot{u}) = p(t) \tag{1}$$

where m, c_v, and k are the mass, viscous damping constant, and stiffness of a structure, respectively; $u, \dot{u}$, and $\ddot{u}$ are the inter-story displacement, velocity, and acceleration of the structure, respectively; f_d and $p(t)$ are, respectively, the friction force of a damper and external loading, which is $-m\ddot{u}_g$ where $\ddot{u}_g$ is the earthquake ground acceleration; sgn$(\dot{u})$ is the symbolic function defined as $-1, 0$ and 1, respectively in case $\dot{u} < 0, \dot{u} = 0$ and $\dot{u} > 0$. To find an exact solution of Eq. (1) is dependent on the form of the external load $p(t)$. It is nearly impossible to obtain an analytical solution for a randomly excited load such as an earthquake, and generally a numerical approach is applied instead. Den Hartog [15] and Hundal [16] provided an analytical solution for Eq. (1) by assuming that the structure with a relatively small friction force shows a steady-state response for harmonic loading. Den Hartog also addressed continuous and stop motion of a mass with combined viscous and Coulomb damping. Hundal found the solution for a structure subjected to a harmonic base excitation. Feeny [17,18] and Liang [19] identified Coulomb and viscous dampings from free-vibration decrements. Previous studies were carried out based on the premise that friction force is small compared to harmonic loading or the structure with a friction damper undergoes free-vibration. If not, the structure behaves with a stop motion and no longer shows harmonic response. In this case a numerical approach should be applied to derive the solution for the equation of motion, which does not give any insight into the vibration characteristics.

This study first revisited previous approaches for identifying a building structure installed with a friction damper under harmonic excitation for reducing steady-state response. By equating the dissipated energy by a friction damper with the energy dissipated by viscous damping for one cycle, a friction damping force can be replaced by an equivalent viscous damping force [20]. As a result, the equation of motion of a single degree of freedom (SDOF) system

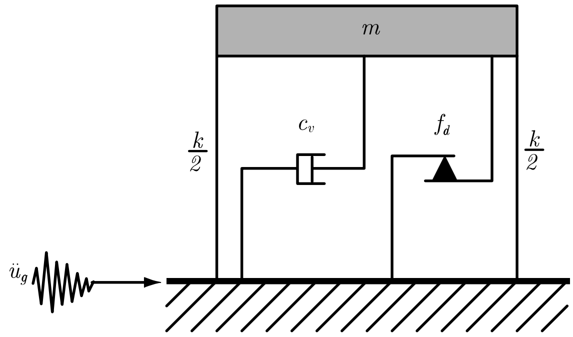

Fig. 1. A single-story structure installed with a friction damper subjected to an earthquake load.

with an equivalent viscous damping subjected to a harmonic force can be represented as

$$m\ddot{u} + (c_v + c_{eq})\dot{u} + ku = F_0 \sin \omega t \tag{2}$$

where c_{eq}, F_0, and ω are the equivalent viscous damping constant, amplitude of harmonic loading, and angular loading frequency, respectively. Eq. (2) can be transformed into the following energy balance equation by multiplying a differential displacement and integrating over the entire displacement [20]:

$$E_K + E_v + E_{eq} + E_S = E_I \tag{3}$$

where E_K, E_v, E_{eq}, and E_S are the kinetic energy, viscously dissipated energy, equivalently dissipated friction energy, and strain energies, respectively; and E_I is the input energy from the external harmonic loading. Since changes in kinetic and strain energies over one cycle are zero for steady-state response, the sum of E_v and E_{eq} over one cycle is equal to the input energy, E_I, which yields

$$\pi(c_v + c_{eq})\omega u_0^2 = \pi F_0 u_0 \sin\phi \tag{4}$$

where u_0 is the amplitude of dynamic displacement and ϕ is the phase angle. The maximum values of the input loading and the output displacement occur with the difference of the phase angle. Expressing Eq. (4) in terms of ξ_v, ξ_{eq} and ω_r leads to

$$2k\pi(\xi_v + \xi_{eq})\omega_r u_0^2 = \pi F_0 u_0 \sin\phi \tag{5}$$

where ξ_v, ξ_{eq} and ω_r are, respectively, the viscous damping ratio, equivalent viscous damping ratio due to friction damping, and the frequency ratio which is the excitation frequency normalized by the natural frequency. The phase angle ϕ is computed as $\phi = \tan^{-1}\frac{2\omega_r(\xi_v+\xi_{eq})}{1-\omega_r^2}$ and thus $\sin\phi$ is obtained as

$$\sin\phi = \frac{2(\xi_v + \xi_{eq})\omega_r}{\left[(1-\omega_r^2)^2 + \{2(\xi_v + \xi_{eq})\omega_r\}^2\right]^{\frac{1}{2}}}. \tag{6}$$

The energy dissipated by a friction damper over a cycle is $4f_d u_0$. Equating this to the equivalent viscous damping energy $\pi c_{eq}\omega u_0^2$ leads to Eq. (7) [20]:

$$\xi_{eq} = \frac{2f_d}{\pi k \omega_r u_0}. \tag{7}$$

Substituting Eq. (6) into Eq. (5) leads to

$$\frac{u_0}{F_0/k} = \frac{1}{\left[(1-\omega_r^2)^2 + \{2(\xi_v + \xi_{eq})\omega_r\}^2\right]^{\frac{1}{2}}}. \tag{8}$$

Since u_0 exists in ξ_{eq}, as shown in Eq. (7), rearranging Eq. (8) leads to the following quadratic equation in terms of u_0:

$$A_1 u_0^2 + 2A_2 u_0 + A_3 = 0 \tag{9}$$

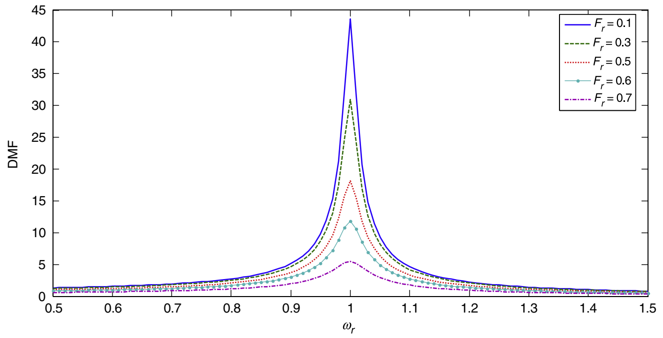

Fig. 2. DMFs with various ω_r's and F_r's when $\xi_v = 0.01$.

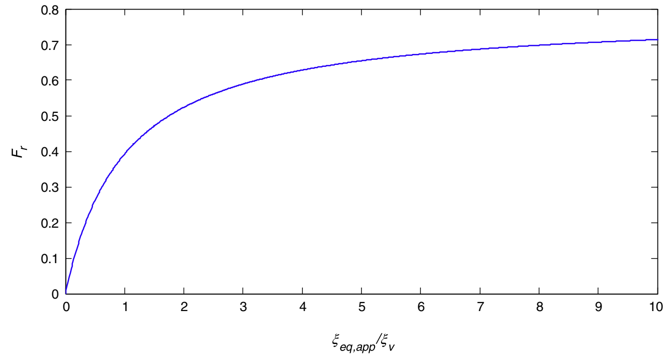

Fig. 3. F_r for various $\xi_{\mathrm{eq,app}}/\xi_v$'s.

where $A_1 = (1-\omega_r^2)^2 + (2\omega_r\xi_v)^2$, $A_2 = \frac{8\omega_r\xi_v f_d}{\pi k}$, and $A_3 = \left(\frac{4f_d}{\pi k}\right)^2 - \left(\frac{F_0}{k}\right)^2$.

Solving Eq. (9) for u_0 and dividing it by the static displacement u_{st}, which is F_0/k, leads to the following form of the DMF:

$$\mathrm{DMF} = \frac{u_0}{u_{st}} = \frac{-\left(\frac{8}{\pi}\right)\omega_r\xi_v F_r + \left[\alpha^2 + 4\omega_r^2\xi_v^2 - \left(\frac{4}{\pi}\alpha F_r\right)^2\right]^{\frac{1}{2}}}{\alpha^2 + (2\omega_r\xi_v)^2} \tag{10}$$

where F_r is the friction force ratio f_d/F_0 and α is defined as $(1-\omega_r^2)$. As u_0 is always positive, the following relationship holds from Eq. (10):

$$\left[\alpha^2 + 4\omega_r^2\xi_v^2 - \left(\frac{4}{\pi}\alpha F_r\right)^2\right]^{\frac{1}{2}} > \left(\frac{8}{\pi}\right)\omega_r\xi_v F_r. \tag{11}$$

Rearranging Eq. (11) leads to

$$F_r < \frac{\pi}{4}. \tag{12}$$

In addition, noting that the term inside the square root in Eq. (10) is always positive leads to

$$F_r < \frac{\pi}{4}\left[1 + \left(\frac{2\omega_r\xi_v}{1-\omega_r^2}\right)^2\right]^{\frac{1}{2}}. \tag{13}$$

Since the right-hand side of Eq. (13) is greater than $\pi/4$, Eq. (12) becomes a governing inequality condition.

As the DMF in Eq. (10) depends on F_r, ω_r and ξ_v, they are illustrated in Fig. 2 with various ω_r's for several values of F_r in the case of $\xi_v = 0.01$. Note that as ω_r approaches 1.0, the magnitude approaches a maximum value for all curves of F_r. The magnitude increases as F_r decreases. As the amplitude of the steady-state vibration is affected by changing the damping ratio, it is expected that F_r takes the role of the damping ratio. In case ξ_v is zero, Eq. (10) is simplified as

$$\mathrm{DMF} = \frac{\left[1 - \left(\frac{4}{\pi}F_r\right)^2\right]^{\frac{1}{2}}}{\left|1-\omega_r^2\right|} \tag{14}$$

which is identical to the form derived by Den Hartog [15]. At resonance, i.e. $\omega_r = 1$, the DMF in Eq. (10) becomes

$$\mathrm{DMF} = \frac{1 - \frac{4}{\pi}F_r}{2\xi_v}. \tag{15}$$

As can be observed in Eq. (15), the steady-state response is guaranteed only when there exists ξ_v. If ξ_v is zero, the DMF becomes infinite, which means that input energy is greater than the energy dissipated by the friction damper.

3. Approximate equivalent viscous damping ratio

The equivalent damping ratio presented in Eq. (7) can be re-expressed as follows using F_r and the DMF:

$$\xi_{\mathrm{eq}} = \frac{2}{\pi}F_r\frac{1}{\mathrm{DMF}}\frac{1}{\omega_r}. \tag{16}$$

Note that the equivalent damping ratio is proportional to F_r and is inversely proportional to the DMF and ω_r. Fig. 2 plots the dynamic magnification factor, DMF, vs. the frequency ratio, ω_r, for various friction force ratios, F_r. Since the DMF is narrow banded with its peak occurring at the natural frequency as observed in Fig. 2, ξ_{eq} in Eq. (16) can be simplified as an approximate equivalent damping ratio $\xi_{\mathrm{eq,app}}$ by using the DMF in Eq. (15) at $\omega_r = 1$:

$$\xi_{\mathrm{eq,app}} = \frac{F_r}{(\pi/4) - F_r}\xi_v. \tag{17}$$

Note that $\xi_{\mathrm{eq,app}}$ is related to both F_r and ξ_v. Rewriting Eq. (17) yields the following equation for the friction force ratio:

$$F_r = \frac{\pi}{4}\frac{\frac{\xi_{\mathrm{eq,app}}}{\xi_v}}{1 + \frac{\xi_{\mathrm{eq,app}}}{\xi_v}}. \tag{18}$$

It can be observed that F_r depends on the ratio of the approximate equivalent damping ratio and the viscous damping ratio, which is $\xi_{\mathrm{eq,app}}/\xi_v$. Fig. 3 shows the relationship between the friction force ratio, F_r, and the ratio of the approximate equivalent damping and the viscous damping. It can be seen that for lower $\xi_{\mathrm{eq,app}}/\xi_v$, F_r increases very rapidly, whereas for larger $\xi_{\mathrm{eq,app}}/\xi_v$, F_r approaches $\pi/4$ asymptotically. Fig. 4 compares the approximate DMF, obtained by substituting $\xi_{\mathrm{eq,app}}$ into Eq. (8) in place of ξ_{eq}, with the DMF obtained using the closed form equation of Eq. (10). It can be noticed that the approximate DMF matches quite well with the exact solution especially when the friction force ratio is small. The discrepancy increases as the friction force ratio increases. However the difference between the approximate and the exact solutions is considered to be acceptable in the preliminary design stage of friction dampers.

Additional equivalent damping ratios contributed by a friction damper are obtained by three methods; Eq. (17) is proposed in this study, closed form DMF using half power band-width method, and approximate DMF using half power band-width method, as shown in Fig. 4. The method using the DMF gives a total damping ratio including viscous damping ratio $\xi_v = 0.01$ inherently in the structure and friction damper contribution. The total damping ratio is also obtained by adding an equivalent damping ratio in Eq. (17) to the viscous damping ratio. The total damping ratios for various values of friction force ratios are compared in Fig. 5. The total damping ratios corresponding to the approximate DMF are quite similar to those obtained by Eq. (17), since both utilize the

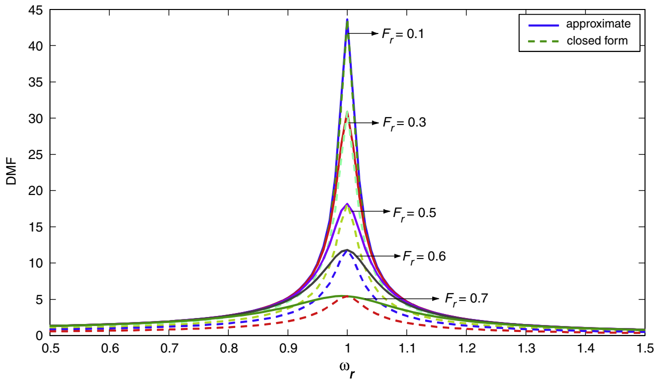

Fig. 4. Closed form and approximate DMFs for several values of F_r when $\xi_v = 0.01$.

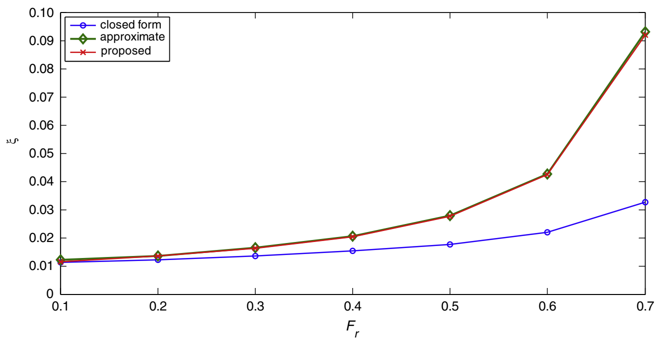

Fig. 5. Comparison of total damping ratios.

same strategy in formulation. They are larger than those obtained using the closed form solution, apparently for larger F_r. This can be explained in Fig. 4 in which the closed form DMF shows a narrower peak than the approximate DMF.

4. Design procedure of a friction damper

To estimate the response of a structure subjected to a random excitation such as an earthquake ground excitation, the frequency contents of the excitation and the transfer function between the excitation and the response need to be known. The mean square response is obtained by integrating the power spectrum of the response over the frequency range of interest, which consists of the multiplication of the transfer function and the power spectrum of the excitation. The behavior of a friction damper is inherently nonlinear and thus its transfer function cannot be obtained. In this study, however, it is assumed that the friction force is small compared with the amplitude of harmonic loading and the steady-state vibration is ensured. Based on this assumption, the approximate equivalent viscous damping ratio is obtained using only the friction force ratio, F_r and the viscous damping ratio ξ_v, as shown in Eq. (17).

Physical insight into response reduction as a result of damper installation can be provided by observing damping ratio rather than friction force contributed by the friction damper. For design purposes, the damping ratio to be supplied by the damper to achieve a target performance, which is denoted as ξ_{target}, can be prescribed regardless of F_r and ξ_v. With this in mind, the amplitude of the dynamic displacement obtained in Eq. (8) can be modified into the following equation using the transfer function, $H(\omega)$, obtained as follows:

$$u_0 = H(\omega) F_0 \tag{19}$$

$$H(\omega) = \frac{1}{k\left[(1-\omega_r^2)^2 + \left\{2(\xi_v + \xi_{\text{target}})\omega_r\right\}^2\right]^{\frac{1}{2}}}. \tag{20}$$

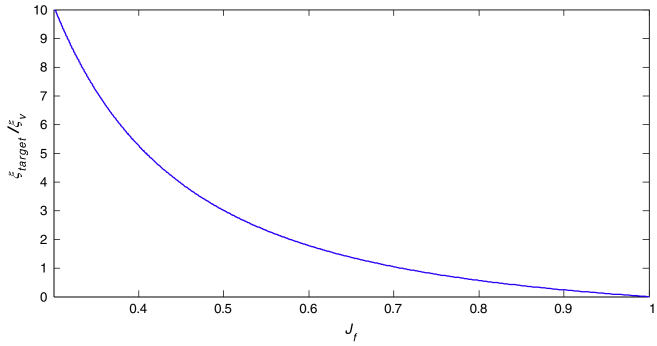

Fig. 6. ξ_{target} for various J_f's.

The right-hand side terms in Eqs. (8) and (20) are almost the same, but their interpretations are different. The former includes magnitude of excitation, F_0 in ξ_{eq}, and therefore cannot be regarded as a transfer function. The latter, however, is considered as a transfer function by prescribing ξ_{target} regardless of F_0.

The mean square displacement is obtained by integrating the displacement power spectrum over all frequency range. For a lightly damped structure, the contribution of the response power spectrum is large in the neighborhood of the natural frequency of the structure, and is very small outside of this frequency region. Based on this observation, the power spectrum of the excitation at the natural frequency can be considered as constant without introducing significant error in the final results [21]:

$$\sigma_f^2 = S(\omega_n) \int_{-\infty}^{\infty} |H(\omega)|^2 \, d\omega \tag{21}$$

where σ_f and $S(\omega_n)$ are, respectively, the mean displacement and the power spectrum of the excitation at the natural frequency, ω_n. Substituting Eq. (20) into Eq. (21) and performing integration result in

$$\sigma_f^2 = \frac{\pi}{2} \frac{S(\omega_n)}{2(\xi_v + \xi_{\text{target}}) m^2 \omega_n^3}. \tag{22}$$

The mean square displacement without a friction damper is easily obtained by substituting zero in ξ_{target}. The vibration control effect of the damper is defined by normalizing Eq. (22) with the mean square displacement obtained without a friction damper and taking a square root, which is

$$J_f = \sqrt{\frac{1}{1 + \frac{\xi_{\text{target}}}{\xi_v}}}. \tag{23}$$

The formulation is based on the assumption that the friction force is small compared with the amplitude of harmonic loading and the relationship between the input force and the output response is linear, which is expressed with the transfer function, $H(\omega)$ in Eq. (20). Tolis and Faccioli [22] utilized a series of earthquake records to obtain reliable structural responses considering the inelastic behavior of a structure. They calculated displacement spectra for various intrinsic damping ratios, which indicates that the damping ratio affects the spectral responses significantly. Since Eq. (23) is obtained by the process that mean square displacement with friction damper is normalized by the mean square displacement obtained without a friction damper, it is governed by the ratio $\xi_{\text{target}}/\xi_v$, not by the intrinsic damping ξ_v. Even though the proposed procedure has the limitation that it does not consider the characteristics of specific earthquakes and dynamic properties of a structure such as the natural frequency and intrinsic damping ratio, the limitation can be compensated for by the simplicity and convenience in designing a friction damper in

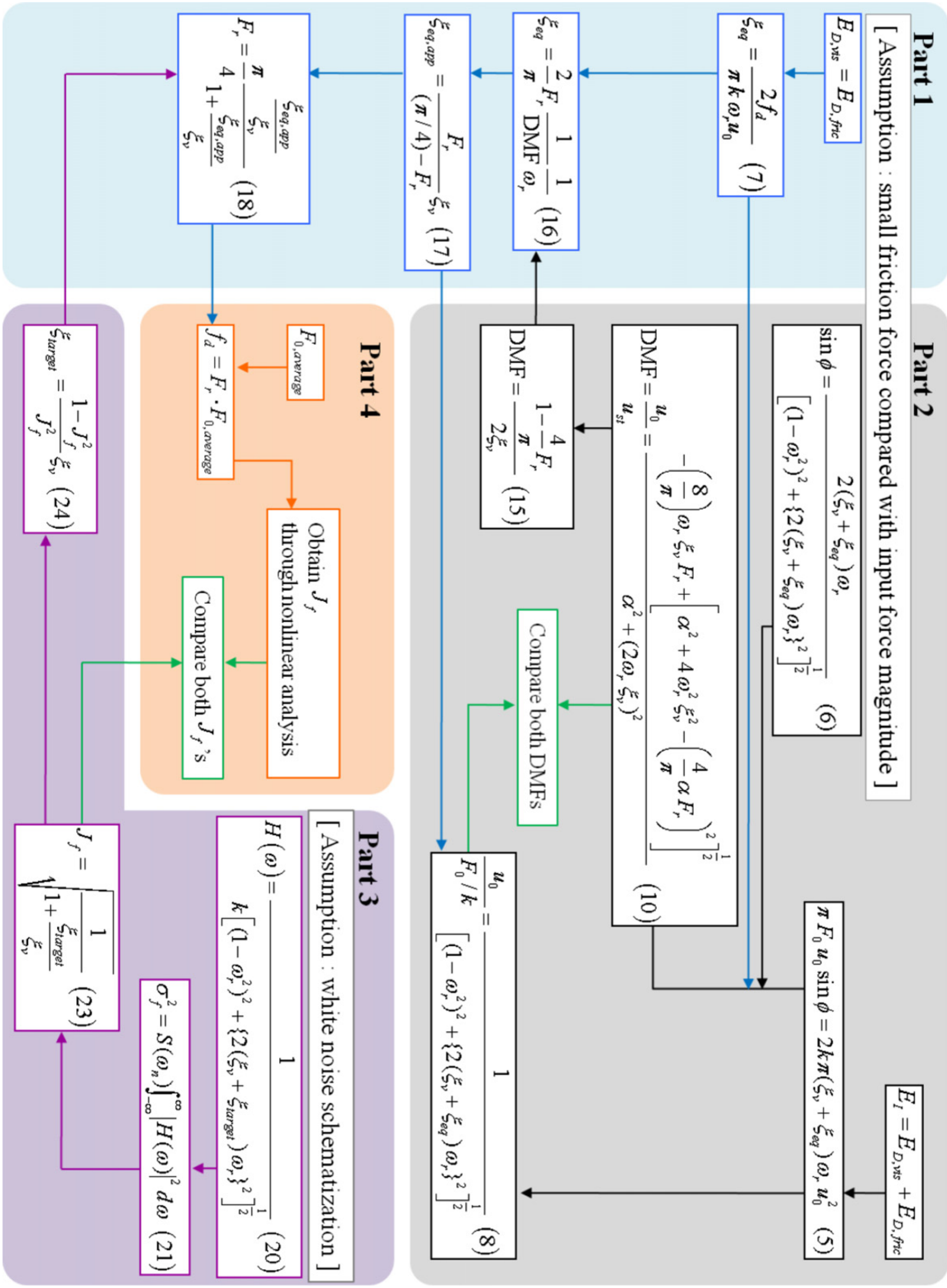

Fig. 7. Flowchart of mathematical derivation procedure and relationship of each part.

the preliminary design stage to achieve a target response reduction factor.

The response reduction factor, J_f, is composed of the ratio of the target damping and the inherent viscous damping ratios. It can be deduced that the displacement response reduction factor presented in Eq. (23) is the same as the response reduction factors for the velocity and the acceleration, since the friction damper affects the damping ratio only. It is appropriate to reorganize Eq. (23) in terms of the response reduction factor to obtain ξ_{target}:

$$\xi_{\text{target}} = \frac{1 - J_f^2}{J_f^2}\xi_v. \tag{24}$$

For the design of a friction damper the response reduction factor is prescribed first and then the corresponding target damping ratio is determined using the above equation.

Generally the larger the damper friction force becomes, the better control performance can be achieved. However, a larger friction force or more friction dampers will lead to higher cost. There has to be a trade-off between cost and control effectiveness. Fig. 6 plots the variation of the target equivalent damping ratio as a function of the response reduction factor. The design of a friction damper is to select a proper friction force required for satisfying a desired control performance. The target effective damping ratio ξ_{target} corresponding to a given J_f can be found in the figure. Once the target damping ratio, ξ_{target} is obtained, F_r is found by using Eq. (18) with ξ_{target} in place of $\xi_{\text{eq,app}}$. The required friction force f_d is then obtained using the relation $F_r = f_d/F_0$, where F_0 is the amplitude of harmonic excitation.

When deriving Eq. (21), the response power spectrum was assumed to be large in the neighborhood of the natural frequency of the structure. For ideal white noise excitation, F_0 is the Fourier transform of the excitation at the natural frequency. For an earthquake excitation, however, its Fourier transform is very irregular along the frequency and therefore it is meaningless to choose F_0 at the natural frequency. Instead, the average of the Fourier transform in the vicinity of the natural frequency is used in this study. As there is no criterion to select proper range of frequency around the natural frequency the half-power points are adopted for identifying bandwidth of frequency for obtaining the average value of F_0, which is denoted as $F_{0,\text{average}}$ [23].

The flowchart illustrated in Fig. 7 summarizes the design procedure for friction dampers, in which the friction force corresponding to a desired response reduction factor can be obtained. The design procedure provided in the flowchart consists of four parts; Part 1 is for the equivalent viscous damping ratio, Part 2 for the DMF, Part 3 for the response reduction factor, and Part 4 for the verification of a designed damper. Each part is connected to one another; for example, the approximate DMF obtained in Part 2 is used to obtain an approximate equivalent viscous damping ratio and friction force ratio in Part 1; the target damping ratio obtained from the response reduction factor in Part 3 is used to obtain the friction force ratio in Part 1; and the amplitude and frequency content of earthquakes and the natural frequency of the structure, which are used for $F_{0,\text{average}}$ in Part 4, are considered in deriving the designed friction force. Thus the four parts are interconnected with each other, as shown in the flowchart.

Eq. (18) provides the friction force ratio expressed with an approximate equivalent viscous damping ratio, which is obtained from Eq. (17). The advantage of these equations is that the relation between friction force ratio (or friction force) and equivalent damping ratio is derived analytically. Eqs. (23) and (24) are derived based on the random vibration strategy for the SDOF structure with the increasing damping ratio of the system. The friction force ratio in Eq. (18) is introduced by substituting the target damping ratio in Eq. (24) into the equivalent damping ratio in Eq. (18). Once the friction force of a damper is found by the proposed procedure, nonlinear numerical time history analysis is performed, and the analysis results for response reduction factors are compared with the target response reduction factors to verify the proposed procedure. The proposed procedure for the design of a friction damper is summarized as the following steps:

Step 1: Select a desired response reduction factor J_f.

Step 2: Obtain target damping ratio ξ_{target} using Eq. (24).

Step 3: Obtain friction force ratio F_r using Eq. (18) with ξ_{target} in place of $\xi_{\text{eq,app}}$.

Step 4: Determine mean values of F_0 and $F_{0,\text{average}}$ considering the natural frequency of the structure and specific earthquake.

Step 5: Obtain a friction force from $F_r \times F_{0,\text{average}}$.

Step 6: (Optional) Verify control performance of the designed friction damper by carrying out nonlinear time history analysis.

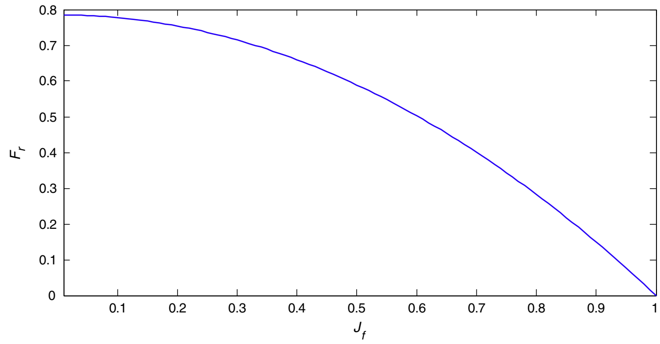

Fig. 8. F_r for various J_f's.

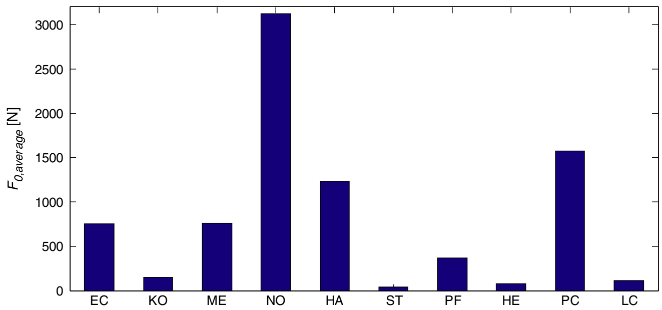

Fig. 9. $F_{0,\text{average}}$ for a single-story structure with $f_n = 0.5$ Hz under 10 seismic records.

5. Verification of the proposed design procedure

The previous section dealt with the process for designing a friction damper to satisfy a given target response reduction factor. The process first began with prescribing a target response reduction factor considering a trade-off between damper cost and control effectiveness. Then the corresponding target equivalent damping ratio was chosen, and finally the required friction force to meet the target performance was obtained. In order to verify the proposed process, numerical time history analysis of a single-story structure installed with a designed friction damper was carried out for 10 seismic records, which are the El Centro (EC), Kobe (KO), Mexico (ME), Northridge (NO), Hachinohe (HA), State Building (ST), Park Field (PF), Helena (HE), Pacomia (PC), and Lytle Creek (LC) earthquakes. The natural frequency of the single-story structure is varied from 0.1 to 1 Hz at intervals of 0.1 Hz. The friction force ratio F_r and the response reduction factor J_f are governed by $\xi_{\text{eq,app}}/\xi_v$ and $\xi_{\text{target}}/\xi_v$, respectively, not by ξ_v as shown in Eqs. (18) and (24), respectively. The proposed procedure begins with the selection of the response reduction factor J_f and the computation of the target damping ratio ξ_{target} which is linearly proportional to ξ_v. In this paper the inherent viscous damping ratio of 0.01 is used throughout the study. Following the proposed step, the friction force ratios are obtained for various response reduction factors, J_f, and are plotted in Fig. 8. The next step is to obtain $F_{0,\text{average}}$ which is defined in this study as the average of the Fourier transform in the vicinity of the natural frequency. Structural seismic response depends on its natural frequency and earthquake excitation, which is considered in computing $F_{0,\text{average}}$. Fig. 9 shows the variation of $F_{0,\text{average}}$ depending on the earthquake records used for input excitation at the natural frequency $f_n = 0.5$ Hz, where f_n is $2\pi\omega_n$. Fig. 10 plots $F_{0,\text{average}}$ of the structure with ten different natural frequencies obtained for El Centro earthquake. The figures show that $F_{0,\text{average}}$ varies depending on both natural frequency and earthquake record.

Once the response reduction factor J_f is given, target damping ratio ξ_{target} can be found using Eq. (24). Then friction force ratio

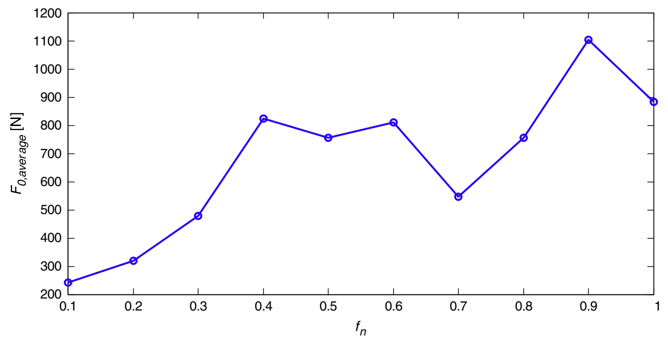

Fig. 10. $F_{0,\text{average}}$ for a single-story structure with various f_n's under the El Centro earthquake.

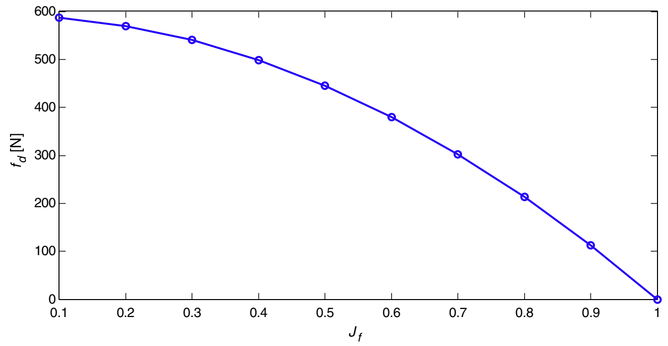

Fig. 11. Designed friction damper forces for a single-story structure with f_n = 0.5 Hz under the El Centro earthquake.

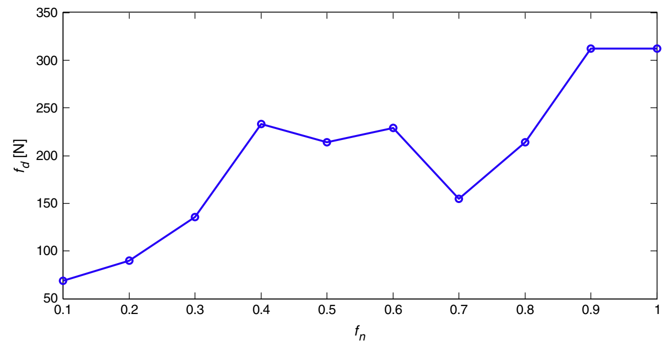

Fig. 12. Designed friction damper forces for a single-story structure with various f_n's and $J_f = 0.8$ under the El Centro earthquake.

is easily found using Eq. (18), which is a function of $\xi_{\text{target}}/\xi_v$, not ξ_{target}. The next step is to determine the friction damper force, which satisfies the target response reduction factor for the structure with a specified natural frequency and earthquake. Fig. 11 shows the designed friction force for the structure with $f_n = 0.5$ Hz under the El Centro earthquake for various response reduction factors J_f. Fig. 12 shows the designed friction force for the structure with $J_f = 0.8$ Hz subjected to the El Centro earthquake as a function of the natural frequency f_n. It can be observed that as the natural frequency increases the designed friction force generally increases.

Fig. 13 present the time history analysis results for displacements and accelerations obtained with and without friction damper. Time history analysis of the model structure was performed for two cases, i.e., for the model without a friction damper ($f_d = 0$), and for the model with the friction damper with f_d = 544.6 N corresponding to the given control ratio $J_f = 0.5$. The structure was modeled using an equivalent mass-spring-dashpot model with $m = 5102$ kg, $\xi_v = 0.01$, and $k = 805.7$ kN/m as

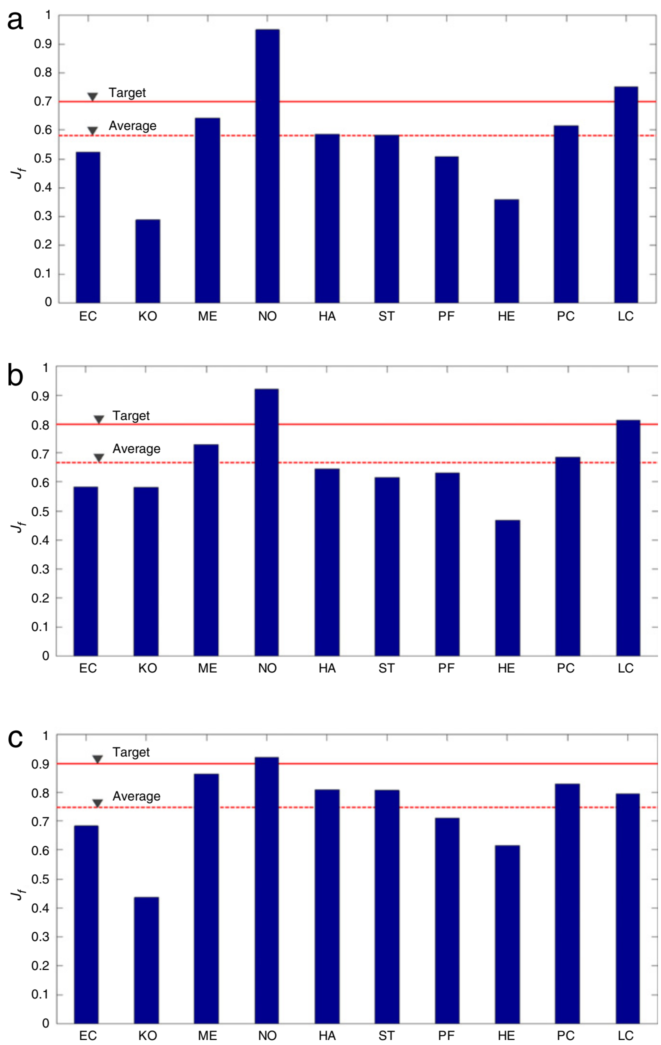

Fig. 13. Response reduction factors for a single-story structure with $f_n = 0.2$ Hz. (a) Target response reduction factor $J_f = 0.7$. (b) Target response reduction factor $J_f = 0.8$. (c) Target response reduction factor $J_f = 0.9$.

the mass, viscous damping ratio, and stiffness for the structure, respectively. The north–south component of the El Centro earthquake was applied for dynamic analysis of the model. The target control ratio J_f of the mean displacement was selected to be 0.5. This led to the target damping ratio and the friction force ratio $\xi_{\text{target}} = 0.03$ and $F_r = 0.589$. The mean value of the Fourier transform of the El Centro earthquake using the half power points was found to be 18.12 gal. The Fourier transform of the excitation in the neighborhood of the natural frequency F_0 was calculated as 924.5 N by multiplying 18.12 gal with the mass of the model. Finally the required damping force f_d is obtained as 544.6 N. It can be observed in the analysis results that the friction damper is effective in reducing both the displacement and acceleration responses.

The response of a structure with friction dampers depends on magnitude of the input earthquake and dynamic properties, especially natural frequency. In order to demonstrate the feasibility of the proposed design procedure of friction dampers, numerical dynamic analysis was performed to obtain response reduction factors. Ten different earthquakes mentioned above were applied for seismic analysis of a single story structure with ten different natural frequencies. Nonlinear time history analysis of Eq. (1) was carried out with $m = 5102$ kg and $\xi_v = 0.01$ with and without the designed friction damper. The equation for the response reduction factor shown in Eq. (23) was derived based on the root mean square

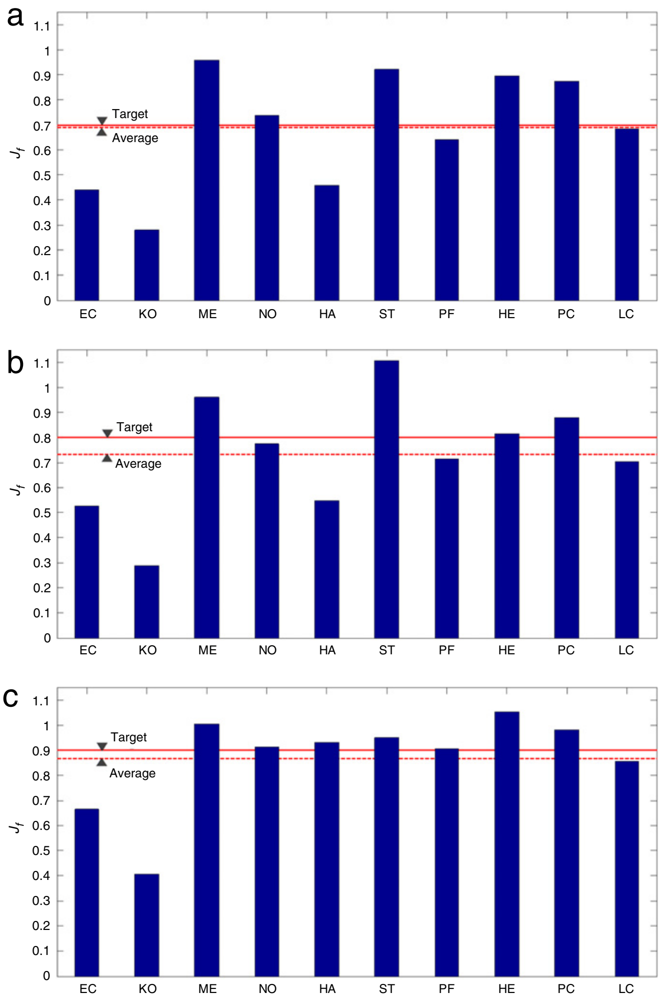

Fig. 14. Response reduction factors for a single-story structure with $f_n = 0.5$ Hz. (a) Target response reduction factor $J_f = 0.7$. (b) Target response reduction factor $J_f = 0.8$. (c) Target response reduction factor $J_f = 0.9$.

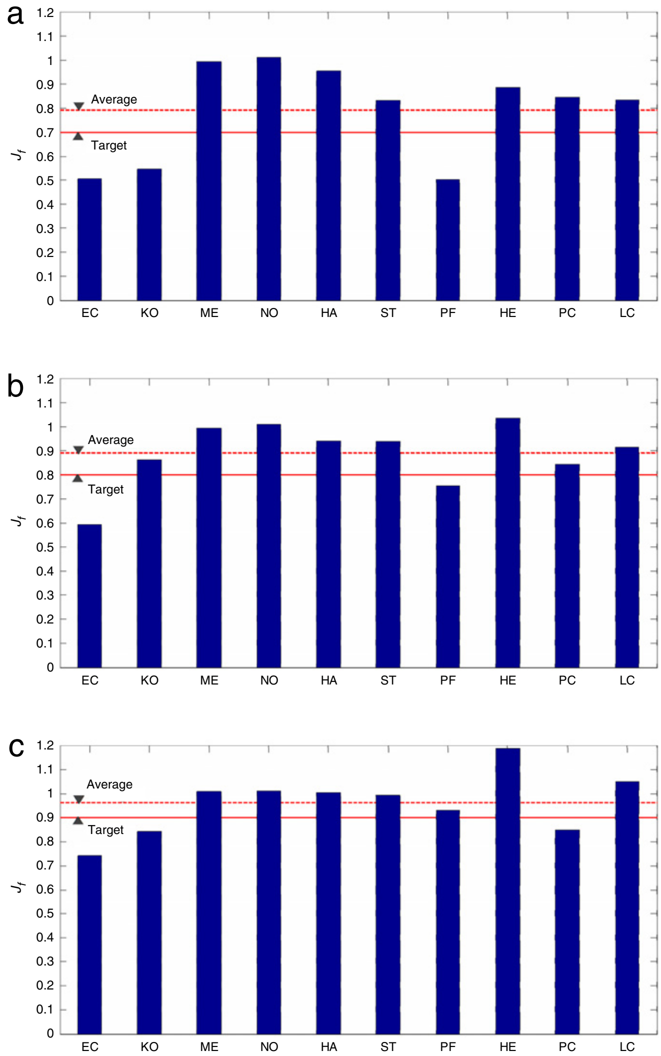

Fig. 15. Response reduction factors for a single-story structure with $f_n = 0.8$ Hz. (a) Target response reduction factor $J_f = 0.7$. (b) Target response reduction factor $J_f = 0.8$. (c) Target response reduction factor $J_f = 0.9$.

of the displacement for stationary random process [21]. Even if temporal mean values were found using only one sample with finite duration, they could be an index to represent control performance. The temporal mean values of the time histories, which were obtained by numerical nonlinear dynamic analysis of the structure with a friction damper, were used in place of the root mean square of responses. The temporal means of the responses of the controlled structure were normalized by those of the uncontrolled one for comparing with the given target response reduction factor. Since the response obtained by using a single earthquake record is not representative from a statistical view point, the response reduction factors obtained by time history analyses using ten earthquake records were averaged and compared with corresponding target factors. Through the analysis the response reduction factors for various target reduction factors, natural frequencies, earthquakes, and viscous damping ratios were obtained.

The structures with natural frequencies $f_n = 0.2, 0.5$ and 0.8 Hz, and inherent damping ratio $\xi_v = 0.01$ subjected to ten earthquakes were analyzed. The friction damper forces were computed for $J_f = 0.7, 0.8$ and 0.9, and the analysis results were illustrated in Figs. 14 and 15. The mean and target values for the response reduction ratio were also shown in the figures. It can be observed in Fig. 14 that a control effect was achieved for most of the earthquake records by installing a designed friction damper in the structure with a natural frequency of 0.2. In the structures with natural frequencies of 0.5 and 0.8 Hz, the mean responses are closer to the target values. However the damper was not so effective for some earthquake records, especially for El Centro (EC) and Kobe (KO) earthquakes, as shown in Fig. 15. This implies nonlinear performance of friction damped structures, where structural response depends on the natural frequency and input earthquake load. However the mean response reduction factors turned out to be close to the target response reduction factors of 0.7, 0.8 and 0.9, respectively. The analysis results demonstrate the feasibility of the proposed simple design procedure to mitigate seismic response of a single story structure. Nonlinearity of the friction damped structure was simplified as a linear one based on several assumptions such as equivalent viscous damping, approximation of the DMF at a natural frequency, and the frequency domain approach using a transfer function.

6. Conclusions

This study presented a simplified design process of a friction damper for controlling seismic responses. A closed form solution for a dynamic modification factor (DMF) was derived by assuming that the friction damped structure showed a steady-state response with a small friction damping force, and that the Coulomb damping force could be replaced by an equivalent viscous damping force. The DMF turned out to be narrow banded and dependent on the equivalent viscous damping ratio at the natural frequency. Based on these observations the equivalent viscous damping ratio was derived from friction force ratio and inherent viscous damping ratio. The equation for the DMF was transformed into a transfer function by adopting the value of the DMF at the natural frequency and rearranging the equation by prescribing target damping ratio. Then response reduction factor of displacement responses with and without friction dampers was found analytically, and a design procedure was proposed to determine the required damper friction force to satisfy a given target response reduction factor. Time history analysis of a SDOF system with a friction damper was carried out to check if the given target response reduction factor was satisfied using ten earthquake records. The analysis results showed that the mean response reduction factors obtained by numerical time history analyses matched well with the target response reduction factors. Based on the analysis results it was concluded that the proposed procedure could be used for designing a friction damper to control structural responses to satisfy a given target performance.

In this study a single-degree of freedom system was used to derive the amount of friction force to meet a given target response. In a multi-story structure with friction dampers installed between stories, the proposed simple process can be applied with the same strategy. First the multi-degrees-of-freedom system needs to be transformed into the equivalent single-degree-of-freedom system. The total amount of friction force is obtained in the modal coordinates of the equivalent system. Then the total amount of the friction force is distributed to each story of the original multi-story structure using appropriate techniques based on modal characteristics of the structure. The process is similar to the capacity spectrum method for the nonlinear static seismic analysis procedure.

Acknowledgements

The work presented in this paper was partially supported by both the Korea Science and Engineering Foundation (KOSEF) grant funded by the Korea government (Project No. 2009-0076304) and the Korean Ministry of Land and the Graduate Research Assistantship of Dankook University.

References

[1] Grigorian CE, Yang TS, Popov EP. Slotted bolted connection energy dissipaters. Earthq Spectra 1993;9(3):491–504.
[2] Li C, Reinhorn AM. Experimental and analytical investigation of seismic retrofit of structures with supplemental damping: part II-friction devices. Technical report NCEER-95-0009. Buffalo (NY): State University of New York at Buffalo; 1995.
[3] Fu Y, Cherry S. Simplified code design procedure for friction damped steel frames. J Struct Eng 1999;116:1334–55.
[4] Fu Y, Cherry S. Design of friction damped structures using lateral force procedure. Earthq Eng Struct Dyn 2000;29:989–1010.
[5] Mualla IH, Belev B. Performance of steel frames with a new friction damper device under earthquake excitation. Eng Struct 2002;24:365–71.
[6] Moreschi LM, Singh MP. Design of yielding metallic and friction dampers for optimal seismic performance. Earthq Eng Struct Dyn 2003;32(8):1291–311.
[7] Bhaskararao AV, Jangid RS. Seismic analysis of structures connected with friction dampers. Eng Struct 2006;28(5):690–703.
[8] Park JH, Min KW, Chung L, Lee SK, Kim HS, Moon BW. Equivalent linearization of a friction damper–brace system based on the probability distribution of the extremal displacement. Eng Struct 2007;29:1226–37.
[9] Lee SK, Park JH, Moon BW, Min KW, Lee SH, Kim JK. Design of a bracing-friction damper system for seismic retrofitting. Smart Struct Syst 2008;4(5):685–96.
[10] Lee SH, Park JH, Lee SK, Min KW. Allocation and slip load of friction dampers for a seismically excited building structure based on storey shear force distribution. Eng Struct 2008;30:930–40.
[11] Lee SH, Min KW, Hwang JS, Kim J. Evaluation of equivalent damping ratio of a structure with added dampers. Eng Struct 2004;26:335–46.
[12] Marko J, Thambiratnam D, Perera N. Influence of damping systems on building structures subject to seismic effects. Eng Struct 2004;26(13):1939–56.
[13] Ribakov Y. Semi-active predictive control of non-linear structures with controlled stiffness devices and friction dampers. Struct Des Tall Special Build 2004;13(2):165–78.
[14] Kim JK, Choi HH, Min KW. Use of rotational friction dampers to enhance seismic and progressive collapse resisting capacity of structures, Struct Des Tall Special Build [in press]. Article first published online: 18 December 2009; doi:10.1002/tal.563.
[15] Den Hartog JP. Forced vibrations with combined Coulomb and viscous friction. Trans ASME 1931;53:107–15.
[16] Hundal MS. Response of a base excited system with Coulomb viscous friction. J Sound Vib 1979;64(3):371–8.
[17] Feeny BF, Liang JW. A decrement method for the simultaneous estimation of Coulomb and viscous friction. J Sound Vib 1996;195(1):149–54.
[18] Feeny BF, Liang JW. Identifying Coulomb and viscous friction from free-vibration decrements. Nonlinear Dynam 1998;16:337–47.
[19] Liang JW. Identifying Coulomb and viscous damping from free-vibration acceleration decrements. J Sound Vib 2005;282:1208–20.
[20] Chopra AK. Dynamics of structures. NJ: Prentice-Hall; 2001.
[21] Crandall SH, Mark WD. Random vibration. NJ: Academic Press; 1973.
[22] Tolis SV, Faccioli E. Displacement design spectra. J Earthq Eng 1999;3(1): 107–25.
[23] Fertis DG. Mechanical and structural vibrations. NJ: Wiley-Interscience; 1995.